Journal of Quantitative Spectroscopy & Radiative Transfer 114 (2013) 109–121

Contents lists available at SciVerse ScienceDirect

Journal of Quantitative Spectroscopy & Radiative Transfer

journal homepage: www.elsevier.com/locate/jqsrt

Resonator spectroscopy of the atmosphere in the 350–500 GHz range

M.Yu. Tretyakov*, M.A. Koshelev, I.N. Vilkov, V.V. Parshin, E.A. Serov

Institute of Applied Physics, Russian Academy of Sciences, 46 Ulyanov Str., Nizhny Novgorod 603950, Russia

ARTICLE INFO

Article history:
Received 31 May 2012
Received in revised form
26 July 2012
Accepted 14 August 2012
Available online 27 August 2012

Keywords:
Microwave spectroscopy
Submillimeter-waves
Accurate laboratory measurements
Atmospheric line parameters

ABSTRACT

Results of studies of the absorption spectra of laboratory air and major atmospheric gases mixed with water vapor in the 350–500 GHz frequency range at atmospheric pressure and room temperature are presented. The spectra were registered for the first time by highly sensitive microwave method employing the resonator spectrometer. Analysis of the spectra allowed determining integrated intensities and values of nitrogen, oxygen and air pressure shift and broadening of the most intense lines of H_2O and O_2 molecules within this range. Some parameters were measured for the first time. The values of parameters were compared with results of earlier measurements and calculations. In addition, a complementary investigation of collisional parameters of the most intense water lines within the considered range by means of the spectrometer with radioacoustic absorption detection at low pressure was performed. Data of these measurements agree with results of analysis of atmospheric spectra within statistical accuracy of both experiments. The research made is important, in particular, for enhancing accuracy of models of radiation propagation in the atmosphere.

1. Introduction

Active mastering of the terahertz frequency range by the atmosphere remote sensing instruments and high diagnostic accuracy requirements stimulate development of radiation propagation models. Model accuracy greatly depends on accuracy of line parameters of atmospheric gases obtained in laboratory studies. Currently, most critical is knowledge of parameters of molecular spectral line pressure broadening and shifting. Multiple limb sounding instruments (e.g., SMLS, ASUR, TELIS, Odin, UARS-MLS, EOS-MLS and SMILES) have recorded narrow range spectra of the atmosphere within the millimeter (mm) and submillimeter (submm) wave range from balloons, airplanes and satellites. Each of these projects has revealed that accurate laboratory parameters are necessary for modeling and extracting environmental data.

In principle conventional Fourier Transform (FT) spectrometer allow analysis of broad-band molecular spectra at THz frequencies. As a good example, Pardo et al. [1] presented the 350–1100 GHz real atmosphere transparency record analysis. However, due to the low sensitivity originating from the lack of bright radiation sources and limited resolution FT spectrometers are not used for the line shape studies especially in the low frequency side of this range. Modern broad-band time domain spectrometers employing short pulse laser radiation converted by a semiconductor to the terahertz range (see, e.g., [2]) can be also mentioned. This fast developing nowadays technique is also still suffering from the lack of sensitivity and resolution sufficient for accurate line shape measurements. As a consequence, most of the laboratory spectroscopic data used for the aforementioned and other remote sensing missions were retrieved from experiments using conventional microwave spectrometers with gas mixtures

* Corresponding author. Tel.: +7 831 4164866; fax: +7 831 4363792.
E-mail address: trt@appl.sci-nnov.ru (M.Yu. Tretyakov).

0022-4073/$ - see front matter © 2012 Elsevier Ltd. All rights reserved.
http://dx.doi.org/10.1016/j.jqsrt.2012.08.019

at low pressure. Typical examples can be found in Refs. [3–6]. Unlike the infrared range where FT spectrometers permit finding parameters of hundreds of lines in a wide range of frequencies and pressures in one experiment, precise investigation of line parameters in the terahertz range is still piece-work. Usually, parameters of one line only are found in one experiment. Therefore, despite a rather long history of mm–submm atmospheric line studies, parameters of diagnostic lines are not known to a presently required accuracy. Moreover, experience shows that a single measurement of line parameters at low pressures typical of spectrometers operating in this range does not guarantee required accuracy due to possible systematic errors. Usage of these data for atmospheric spectra analysis assumes extrapolation of measured values to the range of pressures, which is higher by 2–3 orders of magnitude than the range of measurement.

Measurement of line parameters at atmospheric pressure at well controlled laboratory conditions allows rigorous validation of the low-pressure data. Coincidence of low and high pressure measurement results considerably increases reliability of the data.

The present work is a continuation of a series of studies [7–18] of parameters of the principal diagnostic atmospheric lines of the mm–submm wavelength range by highly sensitive microwave spectrometers, including studies by means of two spectrometers (with complementary capabilities and essentially different principle of operation) based on radioacoustic detection of radiation absorption (RAD) [19] and on the resonator method [20]. The working range of the resonator spectrometer has recently been significantly expanded to the submm wavelengths [21]. This permitted recording at atmospheric pressure of broad-band absorption spectra of air and of two major atmospheric gases (nitrogen and oxygen) mixed with water vapor. The current work presents detailed spectroscopic analysis of these spectra. To the best of our knowledge, such continuous broad-band spectra have not been recorded by means of microwave spectrometers before. In Section 2, we will describe specific features of the resonator spectrometer operation at 350–500 GHz frequencies and of the obtained data. Details of analysis of the spectra will be given in Section 3. Measurements of parameters of the most intense H_2O lines within the considered range at low pressures by means of the RAD spectrometer will be reported in Section 4. Discussion of the results and comparative analysis of data of the new and earlier measurements and calculations will be presented in Section 5 of the paper.

2. The resonator spectrometer and characteristics of the experiment

The broad-band spectra were recorded using the resonator spectrometer and the measurement method analogous to the one employed in our earlier works for registering atmospheric spectra in the 45–96 GHz [11], 130–205 GHz [8] and 285–375 GHz [13] ranges. The spectrometer measures changes in the resonator Q-factor after it has been filled with absorbing gas. The magnitude of these changes is characterized by the change of the resonance response curve width Δf and is related to the absorption coefficient α by (see, e.g., [22])

$$\alpha = -\frac{1}{L}\ln\left(1-\Delta f\frac{2\pi L}{C}\right), \quad (1)$$

where L is the resonator length and C is the speed of light in the studied gas. Note that for small optical depths Eq. (1) becomes independent on L. This feature of the resonator method of absorption measurement gives it a big advantage in comparison with other methods because it excludes systematic errors related to the radiation path length uncertainty, which can be quite large in spectrometers of another type.

The width of resonance response is measured at known frequencies of consecutive longitudinal resonator modes spaced in our experiment by about 300 MHz. The recorded spectrum is equivalent to stepwise recordings in spectrometers with frequency synthesizers. For operation in the 350–500 GHz frequency range, the spectrometer was modified as follows. A backward wave oscillator (BWO tube) of the kind of OB-67 ("Istok", Fryazino, Russia) with an oversized output waveguide having $1.2\times2.4\ \mathrm{mm}^2$ cross-section was used as a generator of radiation. A special quasioptical waveguide system was assembled for resonator excitation. An active frequency multiplier of microwave synthesizer reference signal was employed, which provided a 6-fold reduction of the number of the operating harmonic in the multiplier-mixer of the BWO phase-locked-loop system. A liquid helium cooled InSb bolometer was used as a radiation detector. All changes in the spectrometer and specificity of its operation in the new frequency range were described in detail in the work [21].

The following gas samples were used for our study: (i) the outdoor winter atmospheric air from the compressed air line, (ii) nitrogen gas obtained by evaporation from liquid phase and passed through a flask with doubly distilled water, and (iii) technically grade oxygen with purity better than 98% as declared by the supplier. During the experiment the studied gas was continuously blown through the resonator volume. Manual flow regulator was used. The speed of gas flow was chosen to be 15–20 l/min as a compromise between minimum parasite diffusion of atmospheric gases into resonator chamber and minimum sample consumption. Prior to each recording of the studied spectrum, the spectrometer apparatus function (baseline) was recorded using pure nitrogen as practically non-absorbing gas filling the resonator. All experiments were carried out at room temperature and atmospheric pressure measured by a 600–800 Torr pressure gauge calibrated to an accuracy of 0.5 Torr. Sample temperature and humidity were continuously monitored by a TESTO-645 (Testo GmbH&Co, URL: http://www.testo.de) equipped with highly accurate (as named by the producer) humidity/temperature probe. The guaranteed accuracy of temperature and relative humidity reading in conditions of our study was 0.2 K and 2% RH, respectively. Relative oxygen content in sample was controlled by means of PGK-06-100R gas analyzer with DK-21 sensor ("Insovt", Saint-Petersburg, URL: http://www.insovt.ru/)

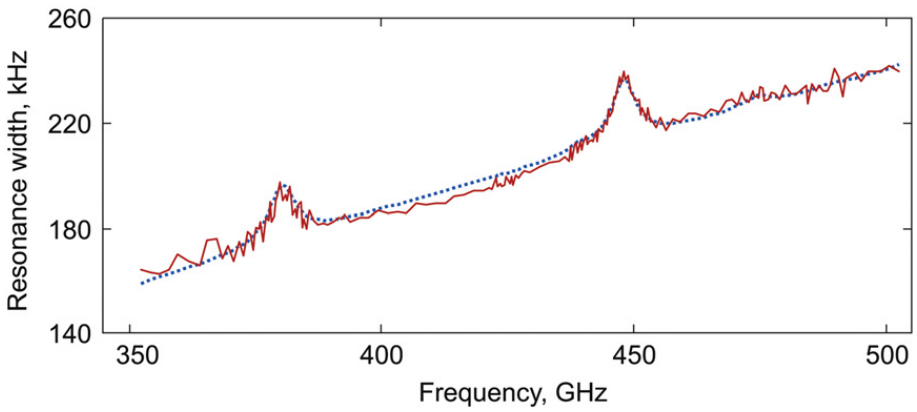

Fig. 1. Resonance response width versus frequency (the spectrometer baseline) for the resonator filled with pure nitrogen. The dotted curve is the calculated dependence with allowance for residual humidity inside the resonator.

with 1% error. Recording of each spectrum and the apparatus function took about several hours. About the same time was necessary for reaching an equilibrium conditions in the resonator chamber before recording the spectrum.

Minor changes of sample absorption caused by temperature, humidity and gas pressure variations during experiments were taken into consideration using modern version of the millimeterwave propagation model (MPM) [23,17] as was described in the work [11]. Note that accuracy of the model is good enough for this purpose because the variations are small and the model gives correct value of the major part of the correction. However to minimize potential systematic related to the model inaccuracy we improved the model and used iterative treatment as described below.

The model was modified as follows: (a) The list of water vapor lines to be taken into account was supplemented with the lines located in the studied frequency range and having maximum absorption exceeding rms value of the spectrometer noise at maximum humidity of the studied samples. These include the ground vibrational state lines of $H_2^{16}O$ corresponding to the transitions $J_{Ka,Kc}=7_{5,3}\leftarrow 6_{6,0}$ (437.3 GHz), $8_{6,3}\leftarrow 7_{7,0}$ (503.5 GHz) and $8_{6,2}\leftarrow 7_{7,1}$ (504.5 GHz); $H_2^{18}O$ $4_{1,4}\leftarrow 3_{2,3}$ (390.6 GHz) and $4_{2,3}\leftarrow 3_{3,0}$ (489.0 GHz) and $HD^{16}O$ $2_{0,2}\leftarrow 1_{1,1}$ (490.6 GHz). (b) For processing the nitrogen and the oxygen experiment spectra, parameters of air-pressure broadening of water lines used in the MPM were replaced by the corresponding parameters of N_2- or O_2-pressure broadening. For the lines whose broadening parameters were not measured, the calculated values from [24] were used. (c) The H_2O–air continuum absorption was increased in factor of 1.12 for the nitrogen, and reduced in factor of 1.73 for the oxygen experiment according to the results of work [25].

One of specific features of studying water vapor lines by the resonator spectrometer is that during the baseline recording it is hard to get rid of residual humidity in the resonator chamber without heating chamber walls, which would result in non-equilibrium conditions of the experiment and so was not used in our work. Water vapor lines are well seen on the baseline, even after many hours of venting the resonator by dry nitrogen when the humidity

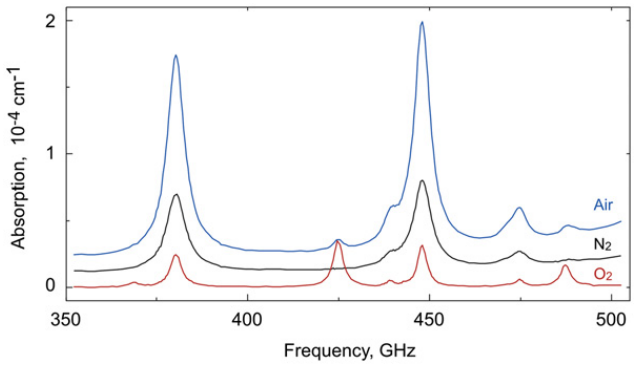

Fig. 2. Spectra of atmospheric air, nitrogen and oxygen mixed with water vapor at room temperature and atmospheric pressure recorded by means of the resonator spectrometer (particular experimental conditions are described in Sections 3.1, 3.2 and 3.3). The N_2 and air spectra are raised up by 10^{-5} and 2×10^{-5} cm^{-1}, respectively, for the picture clarity.

sensor shows a zero value. Fortunately, there are two intense absorption lines of H_2O in the analyzed frequency range. Therefore, sample humidity, as well as its variation during experiment may be determined through known parameters of these lines.

An example of the apparatus function record and the corresponding calculated dependence taking into account the residual humidity are plotted in Fig. 1. Estimates show, that during this recording, the nitrogen humidity was about 110 mg/m^3. The calculated absorption corresponding to residual humidity was subtracted from the baseline spectrum. Value of the absorption constituted on average about 6%, 14% and 70% (for air, N_2 and O_2 records, respectively) of maximal absorption in water lines in the studied frequency range.

The spectra corresponding to an unchanged gas composition and its thermodynamic parameters used in the following analysis are plotted in Fig. 2. Maximal optical depth of the studied samples constituted about 0.08.

3. Analysis of the spectra

Analysis of the spectra implied that gas absorption coefficient $\alpha(\nu)$ in this range may be approximated with a sufficient accuracy by the Van Vleck-Weisskopf

model [26,27]:

$$\alpha(\nu) = I\,N\frac{\nu}{\nu_c}F(\nu), \tag{2}$$

where I is the integrated line intensity normalized by the concentration of absorbing molecules N, ν and ν_c are the current frequency and central line frequency, respectively, and $F(\nu)$ is line shape function normalized by area:

$$F(\nu) = \frac{\nu}{\pi\nu_c}\left(\frac{\Delta\nu}{\Delta\nu^2+(\nu-\nu_c)^2}+\frac{E\nu}{\Delta\nu^2+(\nu+\nu_c)^2}\right), \tag{3}$$

where $\Delta\nu$ is line halfwidth at half maximum. Note that, despite the frequency of observed lines is almost two orders of magnitude greater than their widths, this profile supplies a noticeably smaller standard deviation from experimental data than the Lorentz profile.

A typical feature impeding analysis of all obtained spectra was spectrometer sensitivity to sample humidity that was much higher than the sensitivity of our commercial sensor. This is especially well seen in the O_2 spectrum (Fig. 2). Although the humidity sensor showed zero, like in records of the spectrometer baseline, intense 380- and 448-GHz H_2O lines as well as an order of magnitude weaker lines near 439 and 475 GHz are well seen in the spectrum. Nevertheless, even in that case, the gas humidity assessed by the water lines ($\sim$177 mg/m^3) coincided with sensor indications within allowable error (400 mg/m^3 at 296 K). The 487.3-GHz oxygen line at atmospheric pressure almost coincides with the 488.5-GHz H_2O line that is clearly seen in the air spectrum (Fig. 2). Parameters of this line cannot be found without sufficiently accurate knowledge of gas humidity. Therefore, for determining real humidity during spectra recording we used the 380- and 448-GHz H_2O lines.[1] To minimize related to this possible systematic error, water line intensities in MPM were updated by the most accurate to date results of calculations [28]. The authors of the work [28] guarantee that the intensity calculation error is less than 1% for all the lines. Such a high accuracy and a high (over 100 in all spectra) signal-to-noise ratio in the 380- and 448-GHz lines allow finding gas humidity (as well as related to it water molecule concentration and water vapor partial pressure) with relative error less than 1.5%. This permits calculating with good accuracy values of integrated water line intensities in experimental spectra and use them as fixed parameters in a fit for better determining width and central frequency of H_2O lines poorly resolved and weaker than those near 380 and 448 GHz.

The absorption coefficient was represented as a sum of individual line profiles of corresponding intensities. The contribution of weak H_2O lines near 390.6, 437.3, 489.0 and 490.6 GHz, the contribution of the lines outside studied range, as well as the contribution of the non-resonance (continuum) absorption was calculated by the corresponding MPM version and subtracted from the analyzed spectrum before its further treatment.

The function modeling the observed spectrum was written as

$$M(\nu) = \sum_i \alpha_i(\nu) + A_0 + A_1\nu, \tag{4}$$

where summation is done over all observed (seven H_2O and, if applicable, three O_2) lines. The added function linearly depending on frequency with variable parameters A_0 and A_1 takes into consideration possible inaccuracy of calculating non-resonant absorption in the studied range and minor unaccounted changes of the baseline during long lasting experiments.

Note that analysis of spectra had several iterations. The H_2O line parameters obtained in the course of the work were used for updating the MPM and the processing was repeated.

3.1. N_2+H_2O

Processing of this spectrum was easiest because a minimum number of factors were to be taken into consideration. The gas mixture comprises two components only and only one of them has resonance lines; the composition of this mixture is well controlled and is quite stable throughout the experiment; and the studied gas is least different from the gas filling the resonator during the baseline recording. According to the TESTO indications, the humidity during spectrum recording from the 380-GHz line to the 448-GHz line decreased from 0.39 to 0.37 g/m^3. The most probable reason of this decrease is drift of the sample flow rate. This change agrees well with humidity variations determined spectroscopically using these two lines, but the absolute magnitude of humidity shown by the sensor was 0.31 g/m^3 lower than the humidity found using the lines. Consequently, for calculation of absorption variation during the experiment we used the sensor data increased by 0.31 g/m^3. The residual humidity in the baseline record was found to be 0.105 g/m^3. The total pressure of the mixture during the experiment was 758.5 Torr. The temperature variations were less than 0.3 K at the temperature near 296 K.

The result of spectrum analysis using the function (4) is presented in Fig. 3. Residual of the fit shown in lower part of the figure demonstrates that all influencing factors including variations of parameters during recording, residual water in the baseline, influence of other water lines and the continuum absorption are taken into account to the instrumental noise level and the model function (4) is adequate to the spectrum.

Parameters of line shift δ and broadening γ by N_2 pressure were defined by

$$\delta = \frac{(\nu_c-\nu_0)-\delta_w P_w}{P-P_w} \text{ and } \gamma = \frac{\Delta\nu-\gamma_w P_w}{P-P_w}, \tag{5}$$

where δ_w and γ_w are the self-shift and self-broadening (calculated [29] or measured, if available) of H_2O lines, P is the mixture pressure, P_w is the partial water vapor

[1] The MPM model was used. Humidity is one of the model input parameters. The humidity was varied until minimum difference between observed and calculated spectra was achieved. The method utilizes calculated intensities of many water lines, although the contribution of the 380- and 448-GHz lines is dominant. Therefore the method reveals average over the duration of the experiment value of the humidity.

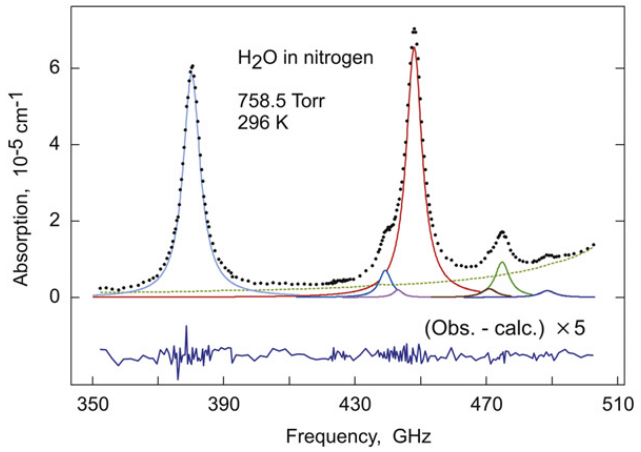

Fig. 3. N_2+H_2O spectrum analysis. Partial water vapor pressure is 0.72 Torr. The thick dots show the experimental spectrum. The calculated profiles of its constituent lines are depicted by smooth solid curves. The smooth dotted curve is for the calculated contribution of the remaining line wings and continuum. Spectrum fitting residual is shown at the bottom.

pressure, and ν_0 is line center frequency measured at low pressure [30].

The found line parameters are listed in Tables 1 and 2.

3.2. Air

According to TESTO indications during spectrum recording, humidity reduced from 1.35 to 1.33 g/m^3. Humidity measurements using the 380- and 448-GHz H_2O lines showed that its change corresponded to the sensor indications, but the absolute magnitude was 0.29 g/m^3 more. Therefore, like in the previous case, indications of the sensor were increased by 0.29 g/m^3. The residual humidity during the baseline recording was found to be 0.11 g/m^3. The total pressure during the experiment was 758.5 Torr. The temperature changes did not exceed 0.2 K near 296 K.

The first triplet of purely rotational O_2 lines near 368.5, 424.8 and 487.2 GHz is located in the considered spectral range. These lines are rather weak and two of them strongly overlap with H_2O lines at atmospheric pressure. Therefore, the spectrum was analyzed in two stages. First, oxygen absorption was calculated by MPM and subtracted from the spectrum. Then parameters of H_2O lines were found like in the previous case. After that, absorption in H_2O lines determined by use of MPM updated by the found parameters was subtracted from the spectrum and the oxygen lines were analyzed.

The atmospheric oxygen spectrum obtained by the aforementioned method is presented in Fig. 4. The figure demonstrates satisfactory (almost to the experimental noise level) subtraction of H_2O lines from the spectrum. The peak intensity of the oxygen triplet's low-frequency line was 6.5×10^{-7} cm^{-1} under our experimental conditions. This line is masked by the spectrometer noise.

The parameters found for H_2O and O_2 line broadening and shift are reported in Tables 1 and 3, and the corresponding intensities are listed in Tables 2 and 4.

3.3. O_2+H_2O

This spectrum is most difficult for treatment. As was mentioned above, the humidity sensor showed the zero value, hence, changes in the mixture humidity could be reconstructed only by H_2O lines and by indirect data on gas flow through the spectrometer chamber. Measurements by lines showed that when the frequency was scanned from 380 GHz to 448 GHz, mixture humidity increased from 0.13 to 0.22 g/m^3. This is in agreement with the situation when before recording the resonator chamber was vented by an intense flow of oxygen (25–30 l/min) down to zero indications of the humidity sensor, after which the flow rate was decreased to reduce gas consumption. It is natural to assume that at a lower flow rate humidity started to grow by an ordinary exponential law due to diffusion of H_2O molecules from the atmosphere until another equilibrium value corresponding to reduced flow rate was established. Thus, we found the empirical dependence of gas humidity on the time of experiment. In addition, during the spectrum treatment it was taken into account that gas temperature varied in the interval from 22.6 to 22.8 °C, and pressure from 741 to 742.5 Torr. The residual nitrogen humidity at baseline recording was 0.116 g/m^3. According to the oxygen sensor indications, the relative concentration of O_2 increased during recording from 98.4% to 100%. Thus it was necessary to take into consideration partial nitrogen pressure, residue of which after baseline recording was continuously displacing under the action of the O_2 flow. This was done at the stage of determining line parameters by introducing the corresponding terms into the expressions for shift and broadening in Eq. (5).

The recorded spectrum, similarly to the previous case, was separated into water vapor spectra in oxygen and oxygen spectrum (Fig. 5). Parameters of the lines found from these spectra are presented in Tables 1–4.

It is worth noting that analyzing this recording we had to make allowance for collision-induced absorption in dry nitrogen (N_2–N_2 continuum) because nitrogen had been used for determining the spectrometer baseline. In two other cases, the nitrogen content in the studied sample was about 79% and 100%. Hence, that component of gas absorption was subtracted from the spectra together with the baseline. The contribution of the dry nitrogen continuum to the observed O_2 spectrum is clear seen on the lower panel of Fig. 5. This trace demonstrates the zoomed-in difference between the absorption in pure oxygen obtained from experimental data neglecting nitrogen continuum absorption in the baseline and the absorption in O_2 calculated by MPM. The smooth solid curve in this part of the figure is for the N_2–N_2 continuum calculated using data of the work [31]. The calculated continuum well corresponds to the systematic difference between observed and calculated spectra. Experimental points are almost uniformly spread above and below the line. If the N_2–N_2 continuum is taken into account the mean value of the residual become very close to zero. Note also that the residual shown in Fig. 5 does not contain any empirical correction presented by A_0 and A_1 coefficients in Eq. (4). The residual demonstrates that (i)

Table 1
Broadening and shifting parameters of studied water lines in MHz/Torr. Experimental uncertainty is given in parentheses in units of the last digit quoted. For the resonator spectrometer results it corresponds to one standard deviation obtained from the fit. For the RAD data the uncertainty also takes into account variations of the parameter value in the repeated measurements.

ν_0 [a], MHz, $J'_{Ka'Kc'} \leftarrow J_{KaKc}$		Oxygen		Nitrogen		Air (measured)		Air (calculated [b])		Water	
		γ	δ	γ	δ	γ	δ	γ	δ	γ	δ
380,197.353(6) $4_{14} \leftarrow 3_{21}$	Res.Sp	2.488(19)	−0.052(11)	4.146(13)	−0.068(6)	3.774(8)	−0.105(5)	3.798(14)	−0.065(7)	–	–
	RAD	2.408(20)	−0.085(18)	4.201(20)	−0.103(13)	–	–	3.824(20)	−0.099(14)	19.20(7)	0.320(40)
	Calc[c]	2.334	−0.112	4.275	−0.150	–	–	3.791	−0.121	25.127	–
439,150.807(9) $6_{43} \leftarrow 5_{50}$	Res.Sp	1.398(63)	−0.073(61)	2.962(50)	0.008(50)	2.699(33)	0.049(27)	2.634(53)	−0.009(41)	–	–
	RAD	1.430(20)	−0.050(15)	3.090(40)	0.100(25)	–	–	2.740(36)	0.068(23)	12.08(5)	0.220(46)
	Calc [c]	1.802	0.073	2.961	0.145	–	–	2.635	0.126	12.978	–
443,018.343(17) $7_{52} \leftarrow 6_{61}$	Res.Sp	1.05(19)	−0.35(19)	2.21(16)	−0.12(17)	2.09(9)	−0.00(10)	1.97(16)	−0.17(17)	–	–
	RAD	1.140(15)	−0.035(15)	2.765(20)	0.245(20)	–	–	2.425(19)	0.186(19)	10.61(2)	−0.305(55)
	Calc[c]	1.669	0.103	2.538	0.276	–	–	2.308	0.215	10.651	–
448,001.085(10) $4_{23} \leftarrow 3_{30}$	Res.Sp	2.093(18)	−0.131(9)	3.851(12)	−0.098(6)	3.449(6)	−0.160(3)	3.482(11)	−0.103(10)	–	–
	RAD	2.110(8)	−0.130(6)	3.847(40)	−0.160(20)	–	–	3.482(33)	−0.154(17)	17.34(3)	−0.820(35)
	Calc [c]	2.166	−0.017	3.896	−0.139	–	–	3.436	−0.108	18.421	–
470,888.889(10) $6_{42} \leftarrow 5_{51}$	Res.Sp	1.51(23)	0.19(24)	3.48(21)	−0.09(22)	2.87(12)	0.07(13)	3.07(21)	−0.03(22)	–	–
	RAD	1.501(45)	−0.028(12)	3.262(30)	0.110(20)	–	–	2.892(33)	0.081(18)	12.93(4)	−0.620(80)
	Calc[c]	1.819	0.081	3.074	0.145	–	–	2.730	0.129	13.648	–
474,689.092(8) $5_{33} \leftarrow 4_{40}$	Res.Sp	1.67(5)	−0.01(5)	3.45(4)	0.03(4)	3.12(3)	−0.06(3)	3.08(4)	0.02(4)	–	–
	RAD	1.745(10)	−0.083(10)	3.530(15)	−0.023(20)	–	–	3.155(14)	−0.036(18)	14.98(6)	−0.96(10)
	Calc[c]	1.966	0.037	3.422	−0.016	–	–	3.014	0.010	15.621	–
488,490.108(9) $6_{24} \leftarrow 7_{17}$	Res.Sp	1.83(29)	0.15(30)	4.18(30)	−0.12(28)	3.48(17)	0.24(20)	3.68(30)	−0.06(28)	–	–
	RAD	2.200(55)	−0.055(25)	3.830(50)	−0.095(50)	–	–	3.488(51)	−0.087(45)	18.10(20)	−0.48(10)
	Calc[c]	2.047	0.042	3.850	−0.0004	–	–	3.369	0.022	19.210	–

[a] Measured by RAD spectrometer in this work.
[b] Calculated from the RAD and the Res.Sp. experimental data assuming 0.79 and 0.21 relative content of N_2 and O_2.
[c] Data are taken from Ref. [24] for O_2 and N_2 and from the latest version of HITRAN [29] for air and for self-broadening.

the MPM is sufficient for calculation the continuum absorption and contribution of water lines outside studied range at conditions of the experiment; (ii) that measured absorption spectra are not biased by some apparatus effect, and (iii) humidity of the sample and its variations are correctly taken into consideration.

4. Low-pressure measurements

Cross-check low-pressure measurements were conducted by a BWO-based spectrometer with frequency synthesizer and radioacoustic detection of absorption (RAD spectrometer [19,32]). In the present work collisional parameters of H_2O lines near 439, 443, 448, 470, 474 and 488 GHz were measured for the first time. Besides, a more extensive study (compared to [13]) of pressure shift and broadening by different gases [33], including H_2O, N_2 and O_2, was carried out for the 380-GHz line. Parameters of shifting and broadening by pressure of water vapor, nitrogen and oxygen lines were measured at room temperature in the interval of pressures from 0.2 to 4 Torr. Vapor of doubly distilled water mixed with nitrogen or oxygen with purity better than 99.99% were used as experimental samples. Gas mixture pressure was continuously monitored during the experiment using MKS baratron gauge (Type 627-B of 10-Torr range) with 0.12% accuracy as declared by the producer. Data of major experimental conditions are given in Table 5. Details of measurements of H_2O line parameters by the RAD spectrometer can be found in the papers [15,18].

The shape of the observed lines was analyzed by the Voigt profile. A typical example of the record of the observed line and its fitting residual is shown on the right panel of Fig. 6. For comparison, the result of analysis of the shape of this line by the Van Vleck-Weisskopf profile at atmospheric pressure is given on the left panel of the figure.

Fig. 6 clearly demonstrates complementary abilities of the resonator and the RAD spectrometers. The 380-GHz line records made by these two spectrometers at pressures differing by more than four orders of magnitude look very similar. The signal to noise ratio in both cases is several hundred, providing high statistical accuracy of line parameter measurements. A large difference in pressure allows rigorous verification of measured values of line collisional parameters, which should linearly depend on pressure. Minor systematic deviations of the low-pressure recording fit residual demonstrate the well-known failure of the Voigt profile in reproducing high quality experimental data (see, e.g., [34] and references therein). Many sophisticated models have been proposed for an adequate modeling of the molecular line profiles including in particular shape of water lines (most extensive recent

Table 2
Integrated intensities of water lines in 10^{-22} cm/molecules. Experimental uncertainty corresponds to one standard deviation obtained from the fit.

	Meas. in O_2	Meas. in N_2	Meas. in air	Calc.[a]
380 GHz, $4_{14}\leftarrow3_{21}$	8.292(54)	8.272(29)	8.349(16)	8.280
448 GHz, $4_{23}\leftarrow3_{30}$	8.579(68)	8.644(29)	8.596(15)	8.651

[a] Ref. [28].

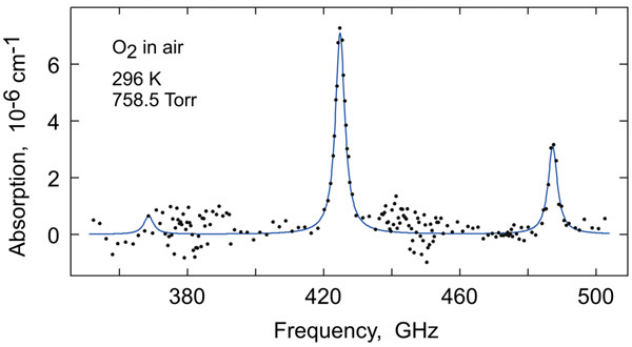

Fig. 4. Dots—absorption in dry atmospheric air determined from experimental data. Solid curve—spectrum of oxygen in air calculated by MPM.

Table 4
Integrated intensities of studied $^{16}O_2$ lines in 10^{-25} cm/molecules. Experimental uncertainty corresponds to one standard deviation obtained from the fit.

Frequency, $N'J'\leftarrow NJ$	Meas. in O_2	Meas. in air	HITRAN
368 GHz, 3,2←1,1	0.226(12)	–	0.2224
425 GHz, 3,2 ←1,2	2.500(11)	2.437(10)	2.425
487 GHz, 3,3←1,2	1.08(11)	1.00(10)	1.036

Table 3
Broadening and shifting parameters of studied oxygen lines in MHz/Torr. Experimental uncertainty for the resonator spectrometer results corresponds to one standard deviation obtained from the fit. For the RAD data the uncertainty also takes into account variations of the parameter value in the repeated measurements.

		368 GHz		425 GHz		487 GHz	
		γ	δ	γ	δ	γ	δ
O_2	Res.Sp.	2.25(16)	0.049(97)	2.181(14)	0.015(7)	2.139(30)	0.025(17)
	RAD [a]	2.256(30)	–	2.191(10)	–	2.106(30)	–
	HITRAN	1.838	–	1.740	–	1.740	–
Air	Res.Sp.	–	–	2.136(67)	0.010(67)	1.93(30)	0.008(79)
	RAD [a]	–	–	2.211(18)	–	2.163(85)	–
	HITRAN	1.874	–	1.775	–	1.775	–

[a] Data from work [9] were recalculated to 296 K using MPM's temperature exponent $n=0.8$.

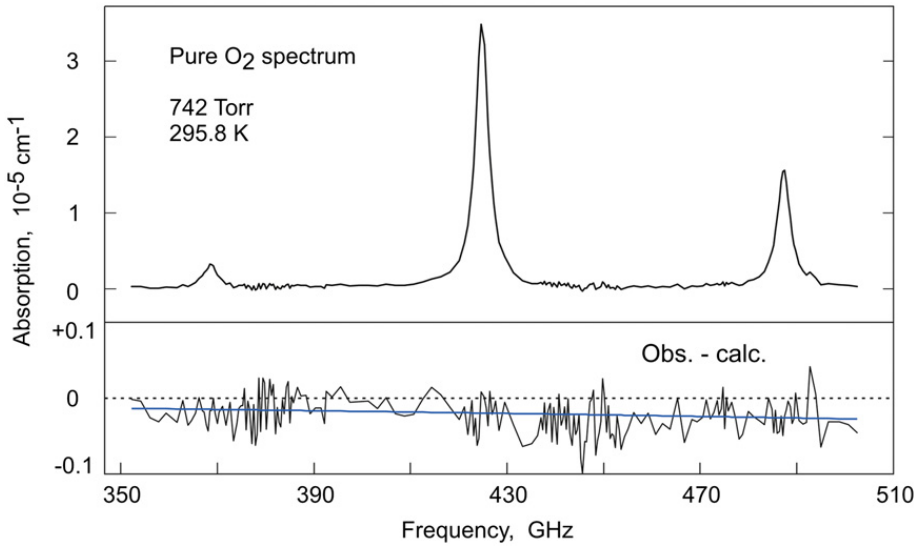

Fig. 5. Oxygen spectrum obtained by subtracting water lines from experimental data. At the bottom—difference between O_2 spectrum obtained neglecting nitrogen continuum absorption in the baseline and spectrum calculated by MPM. The smooth solid line on the lower panel corresponds to N_2–N_2 continuum calculated using data of [31].

Table 5
Experimental conditions during the low-pressure study of water lines by the RAD spectrometer.

Line	Perturbing molecule	Path length (cm)	Partial pressure (Torr)		T (°C)	Number of experiments
			Water vapor	N_2/O_2		
439 GHz, $6_{43}\leftarrow5_{50}$	H_2O	10	0.21–1.51	–	24.0	1
	N_2/O_2	10	0.05–0.21	0.26–3.94	22.0–23.5	4/3
443 GHz, $7_{52}\leftarrow6_{61}$	H_2O	10	0.32–1.54	–	23.5	1
	N_2/O_2	10	0.15–0.25	0.25–2.88	21.5–24.4	3/3
448 GHz, $4_{23}\leftarrow3_{30}$	H_2O	10	0.05–1.32	–	22.4	1
	N_2/O_2	10	0.01–0.15	0.20–3.00	23.5–24.0	2/4
470 GHz, $6_{42}\leftarrow5_{51}$.	H_2O	10	0.09–1.52	–	22.5–25.0	2
	N_2/O_2	10	0.05–0.15	0.25–4.23	23.0–25.5	4/5
474 GHz, $5_{33}\leftarrow4_{40}$	H_2O	10	0.09–1.82	–	22.4–25.5	3
	N_2/O_2	10	0.04–0.13	0.15–3.87	24.5–27	2/2
488 GHz, $6_{24}\leftarrow7_{17}$	H_2O	10	0.17–1.81	–	24–25	2
	N_2/O_2	10	0.09–0.21	0.30–3.92	23.0–25.5	2/2

review can be found in Ref. [35]. It is worth mentioning that the use of, for example, the speed dependent (SD) Voigt profile would eliminate these deviations by the cost of one more adjustable parameter. However, the collisional line width determined from the SD Voigt profile and having a clear physical meaning does not exactly correspond to the ad hoc parameter of collisional line width (note the same name) in the Voigt, Lorentz, Van Vleck-Weisskopf and other similar traditional profiles. It was shown for various molecules (see, e.g., [36] and references therein) that use of the SD Voigt profile results in systematically larger collisional width in comparison with the Voigt profile. Therefore, mistaken use of the simple conventional line shape models with the line width determined using the SD Voigt profile would lead to systematic error in absorption calculations of the order of several percent. This work is mainly aimed at providing atmosphere remote sensing community by accurate laboratory data. Most of modern radiation propagation models employ traditional line profiles, which have an advantage of a fast spectra computing. Therefore, in spite of recognition of definitely higher accuracy of the SD-Voigt, we refrain using the model in this work leaving it for further studies.

Fig. 7 demonstrates changes in the width and observed central frequency (in fact, the line shifting is negative, which is impossible to present on logarithm scale, so only the absolute value of the shift is shown) of the 380-GHz line with variation of partial pressure of perturbing gas. Broadening and shifting parameters were determined as a linear regression of the low pressure experimental points. Note than points obtained from atmospheric pressure experiments were not included in the fit. It is really astonishing that the 300× extrapolation of the low-pressure measurement (shown in Fig. 7 by straight solid lines) falls in such close vicinity to the result obtained by means of the resonator spectrometer at atmospheric pressure.

The found line parameters are listed in Table 1. All the parameters of line broadening presented in the table were recalculated for the temperature of 296 K for correct comparison. The calculations were made by the empirical

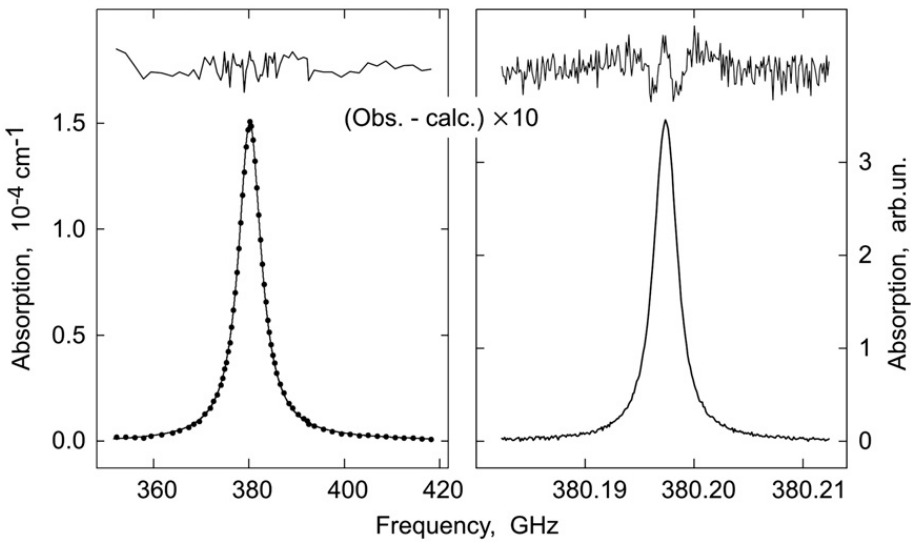

Fig. 6. Left: 380-GHz water line recorded by resonator spectrometer in laboratory air (partial water vapor pressure 1.67 Torr, total pressure 758.5 Torr, temperature 296 K). The smooth solid line corresponds to the Van Vleck-Weisskopf profile fitted to the experimental points (shown by circles). Collisional line width determined from the fit is 2891(7) MHz. The fit residual enlarged by a factor of 10 is shown above. Right: the same line recorded by RAD spectrometer in pure water vapor at 56 mTorr and 297 K. Residual of the Voigt profile fitted to the line is shown above the record. Collisional line width determined from the fit is 1.068(3) MHz.

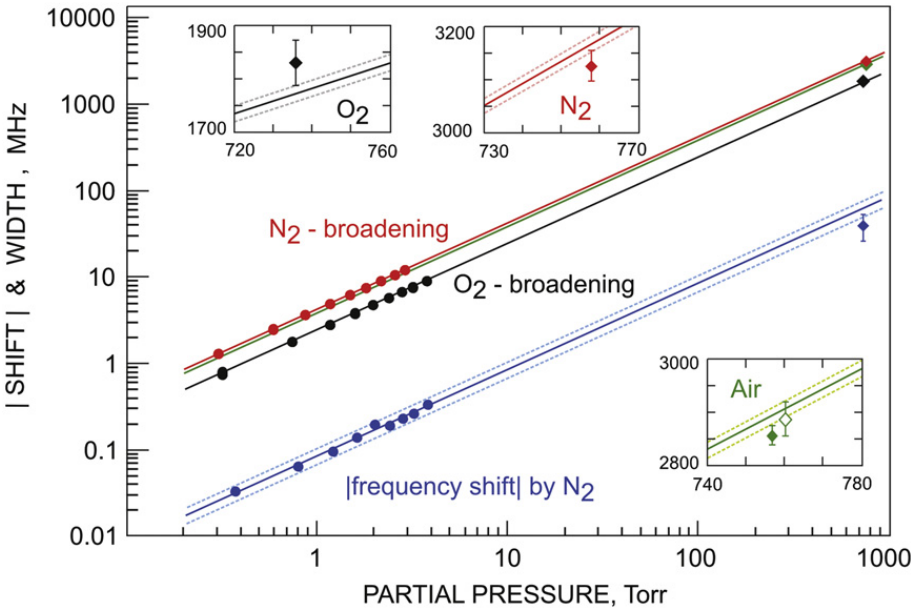

Fig. 7. Pressure shift and broadening of the 380-GHz H_2O line. Red—nitrogen broadening, black—oxygen broadening; blue — absolute value of negative nitrogen pressure shift of the line center frequency; circles—RAD measurements; filled diamonds—obtained from the atmospheric pressure spectra recorded by the resonator spectrometer; green—dry air broadening, empty diamond—calculated from the N_2- and O_2 – experimental data assuming 0.21/0.79 ratio of the O_2/N_2 relative content in air; solid lines—results of linear approximation of the low pressure measurements; dim dotted lines correspond to experimental uncertainty of RAD measurements; green solid line—calculated air broadening by RAD data. Zoomed-in fragments of the plot nearby the resonator spectrometer results are shown in inserts on linear scale Statistical error of measurements by resonator spectrometer presented by the vertical bar corresponds to 3σ. (For interpretation of the reference to color in this figure, the reader is referred to the web version of this article.)

power dependence $\gamma(T)=\gamma(T_0)(T/T_0)^n$ with $n=-0.75$ for all lines. Error caused by the difference between this approximate temperature exponent and the true one for each line (which is actually unknown) is negligible in comparison with the statistical measurement accuracy, as temperature changes between different experiments did not exceed 2–3 K. Parameters of shift were not recalculated to the uniform temperature as their temperature dependence is unknown.

Note that study of the 439-GHz H_2O line revealed that shifts of its center frequency by N_2 and O_2 pressure are different not only in magnitude, but in sign too. As such a behavior had not been observed for other lines, we cross-checked parameters of this line using a specially prepared mixture of nitrogen and oxygen. Partial N_2 and O_2 pressure (2.776 and 5.665 Torr, respectively) in the mixture was chosen so that the shift of water line center frequency should be close to zero. The measured values of

broadening and shift by such a mixture (1.970(15) and +0.002(10) MHz/Torr at 24.2 °C) agree well with the expected values (1.971(27) and −0.000(18) MHz/Torr), which may be obtained from the data presented in Table 1. This trial confirms high accuracy of the conducted measurements.

5. Discussion

Comparative analysis of collisional parameters of the studied lines (Tables 1, 3 and Figs. 8–10) shows that nearly all broadening and shift parameters determined from the atmospheric spectra agree, within statistical error, with the data obtained at low pressure. The exception is the 443-GHz H_2O line, which is hardly seen in the atmospheric spectra. The same agreement is observed between the parameters of H_2O lines directly retrieved from the air spectrum and the parameters calculated from the corresponding data retrieved from the N_2- and O_2-spectra assuming 0.21/0.79 O_2/N_2 relative content of the air (Table 1 and the lower part of Figs. 10–11).

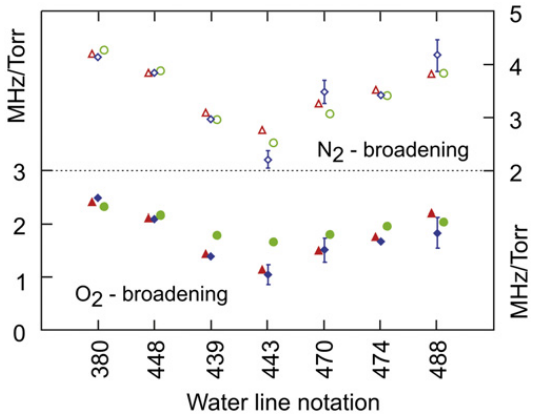

Fig. 8. Comparison of measured in this work and calculated in [24] broadening parameters. Upper panel (open symbols, right scale) corresponds to nitrogen and lower panel (filled symbols, left scale) to oxygen. Approximate line frequency in GHz is used for line notation. Red triangles correspond to measurements by RAD spectrometer; blue diamonds—by resonator spectrometer; green circles—results of calculations [24]. Symbols corresponding to each line are slightly shifted from each other along *OX* axis for figure clarity. Error bars are shown in correspondence with Table 1. The bar is not shown if its value is less than the symbol size. (For interpretation of the reference to color in this figure, the reader is referred to the web version of this article.)

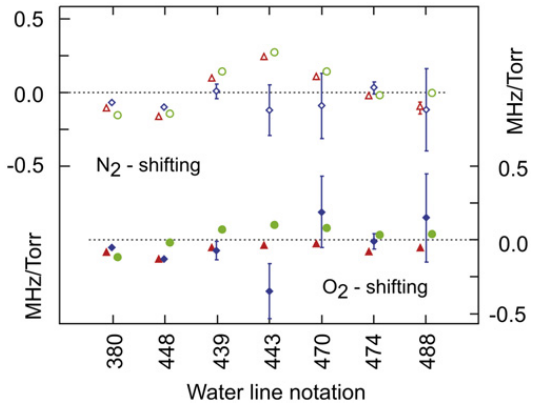

Fig. 9. Comparison of measured in this work and calculated in [24] shifting parameters. Upper panel (open symbols, left scale) corresponds to nitrogen and lower panel (filled symbols, right scale) to oxygen. Approximate line frequency in GHz is used for line notation. Red triangles correspond to measurements by RAD spectrometer; blue diamonds—by resonator spectrometer; green circles—results of calculations [24]. Symbols corresponding to each line are slightly shifted from each other along *OX* axis for figure clarity. Error bars are shown in correspondence with Table 1. The bar is not shown if its value is less than the symbol size. (For interpretation of the reference to color in this figure, the reader is referred to the web version of this article.)

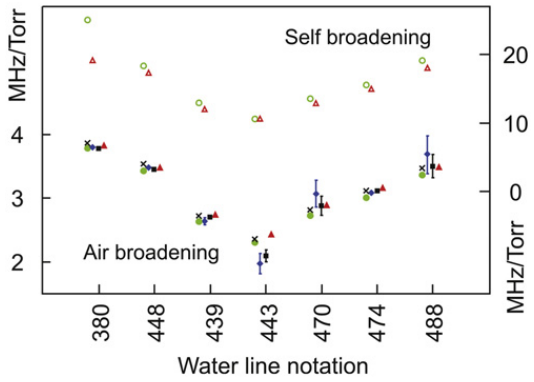

Fig. 10. Comparison of dry air pressure broadening parameters of several water vapor lines measured in this work and taken from HITRAN database (lower part, left scale, filled symbols) and self-broadening (upper part, right scale, open symbols). Approximate line frequency in GHz is used for line notation. Red triangles correspond to measurements by RAD spectrometer; black squares—by resonator spectrometers, blue diamonds—calculated from the resonator spectrometer data obtained from the O_2- and N_2-experiments; green circles—data from HITRAN; crosses—calculated from O_2 and N_2 broadenings obtained by the CRB method [24]. Symbols corresponding to each line are slightly shifted from each other along OX axis for figure clarity. Error bars are shown in correspondence with Table 1. The bar is not shown if its value is less than the symbol size. (For interpretation of the reference to color in this figure, the reader is referred to the web version of this article.)

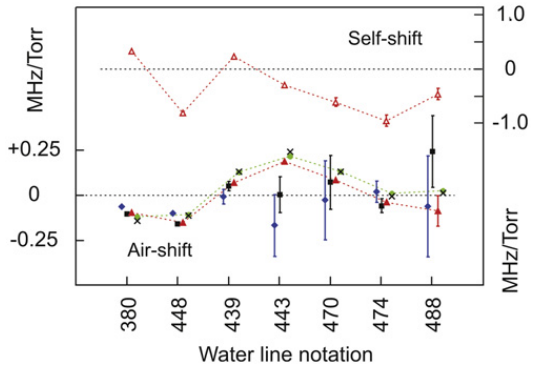

Fig. 11. Data on air (filled symbols, left scale) and self-shift (empty symbols, right scale) of water lines considered in this work. Approximate line frequency in GHz is used as line notation. Red triangles correspond to measurements by RAD spectrometer; black squares—by resonator spectrometer; blue diamonds—calculated from nitrogen and oxygen atmospheric spectra recordings assuming 0.21/0.79 relative content of O_2/N_2. Green circles—data from HITRAN. Crosses—calculated from O_2 and N_2 shifts obtained by the CRB method [24]. Symbols corresponding to each line are slightly shifted from each other along *OX* axis for figure clarity. Error bars are shown in correspondence with Table 1. The bar is not shown if its value is less than the symbol size. (For interpretation of the reference to color in this figure, the reader is referred to the web version of this article.)

Such agreement evidences that systematic errors are minimized to the level of statistical uncertainty.

It is interesting to compare the found water line parameters with the results of the most accurate to date theoretical calculations [24] using the complex Robert-Bonamy (CRB) method. Note that some problems associated with this approach have been recently discussed by Ma et al. [37] The comparison demonstrates a good agreement. Deviation of the calculated N_2 and O_2 pressure broadening parameters from the experimental ones varies within 1.2–9% and 2.5–30%, respectively (Fig. 8). However, these discrepancies amazingly compensate each other and the air-broadening parameters calculated from these data agree with the results obtained from the RAD measurements within 1–3%. The air-broadening data from the HITRAN database are systematically lower than the CRB data by about 2–3% and demonstrate a little larger but still insignificant deviation from the experimental data (the lower part of Figs. 10 and 11). A larger relative deviation of the HITRAN data is observed for the self-broadening data, which increases up to 24% for the 380-GHz line (the upper part of Fig. 10).

Discussion of pressure lineshifts is of special interest. The shifts are very difficult to calculate accurately especially for lines of molecule such as H_2O, which requires knowledge of anisotropic potential taking into account long range multipole electrical interactions as well as short range interactions. In the CRB method broadenings and shifts are calculated together because both are result of molecular collisional interaction. The broadening is the largest collisional effect, so it is less sensitive to inaccuracies of the theoretical model than the shift. Usual comparative analysis of relative values in the case of shift does not give much information because absolute values are rather small, moreover, measured and calculated shifts may be different in sign. Nevertheless, Figs. 9 and 11 where measured and calculated shifts are plotted versus line number (which is analogous to the transition quantum numbers), clearly demonstrate that the calculated and measured shifts are of the same order of magnitude. Moreover, they have a similar dependence on the line number, which confirms that modern methods of calculations are capable to make good estimation of the shifts. In Fig. 11, the CRB calculations [24] of air shifts are compared with the experimental data and with the data from the HITRAN database. Correct general behavior of calculated data should be pointed out once again. Note that pressure shifts of several tens of kHz/Torr are discussed with good grounds in this work, which is, as far as we know, the first case in the history of line shift studies when such a small shift measurement is confirmed by another independent measurement and by theoretical calculations.

Note also a good agreement between the results of measurements of nitrogen and oxygen pressure shift and broadening of the 380-GHz line and the results of studying parameters of this line at low pressure on a different setup of the RAD spectrometer [13]. Results of these two measurements are collected in Table 6. Note that in Ref. [13] the data are given for 25 °C. The N_2- and O_2-broadening and shifting parameters as well as the self-shifting agree within given uncertainties with the new data (Table 1). Difference between old and new shifting coefficients does not exceed 5 kHz/Torr. The discrepancy of the self-broadening parameter that is beyond estimated error is explained by neglect of the value of optical depth of gas in the cell during data processing done in our previous work. More exact is the new value of self-broadening parameter 19.20(7) MHz/Torr that is smaller than our earlier data [13] by about 2%.

Table 6
Broadening and shifting parameters (in MHz/Torr) of the 380-GHz water line at 296 K measured by us using different setups of the RAD spectrometer in this work and in 2006 [13].

Perturber	Broadening		Shifting	
	This work	Ref. [13]	This work	Ref. [13]
O_2	2.408(20)	2.433(30)	−0.085(18)	−0.082(6)
N_2	4.201(20)	4.233(30)	−0.103(13)	−0.098(6)
H_2O	19.20(7)	19.61(1)	+0.320(40)	+0.315(20)

Unshifted positions of water lines obtained as by-product of line center shifting measurements by the RAD spectrometer (Table 1) agree within statistical uncertainty with results of study of these lines by the Lamb-dip method [30]. The deviations vary from −20 up to +12 kHz confirming high accuracy of the study.

Integrated intensities of all O_2 lines measured by means of the resonator spectrometer in experiments with oxygen and air (Table 4) exceed the HITRAN [29] and GEISA [38] data by 2–4%. This difference agrees with the fact that, during analysis of the atmospheric spectra, the oxygen spectrum calculated by the MPM, which uses line intensities from HITRAN, could be subtracted completely (to the level of experimental noise) only when the calculated absorption was increased by 2–2.5%. The obtained data indicate that the calculated intensity of rotational lines of the studied O_2 triplet is underestimated in the available databases.

Analysis of oxygen spectrum confirmed that the frequency shift of O_2 lines by nitrogen and oxygen pressure is negligibly small. The use of line center frequencies measured at low pressure as fixed parameters for O_2 spectrum fitting did not give pronounced changes in the found values of width and intensity of the observed lines.

It is worth noting that the broadening parameters of oxygen lines in the HITRAN and GEISA databases differ from the experimental values up to 20%. These data have not been updated for many years, although values of the parameters are known from experiment to an accuracy of ~1% [9].

Despite the fact that gas humidity during recording the atmospheric spectra was determined by the calculated values of intensity of the 380- and 448-GHz H_2O lines, analysis of their integrated intensities allows assessing accuracy of these calculations. Method of water line intensity measurements used in this work cannot reveal any systematic under- or overestimation of calculated intensities. However it allows analyzing variations of calculated intensities from some average value. Note that due to the specific of measurements described in

Sections 2 and 3 the mixture humidity was slightly growing in experiments with nitrogen and oxygen and was reducing in experiment with air. Nevertheless, the observed integrated intensity of the 380-GHz line is a little more and of the 448-GHz line a little less than the calculated value almost in all cases. The difference is within 0.6–0.8%. This is only slightly higher than a weight-average measurement error, but is much higher than the statistical error of the intensity measurements in experiments with air, where humidity, hence, signal-to-noise ratio in water lines was maximal. Thus, the data obtained do not contradict the 1% declared accuracy of calculations, but show that the real accuracy is not significantly higher than the declared one.

Parameters of water-related non-resonant absorption have not been investigated in this work, primarily because its contribution is negligible at low humidity of the studied gases. Analysis has demonstrated that the continuum absorption in the conditions of the considered experiment may be calculated by the MPM model to an accuracy of spectrometer noise. However, it is worth pointing out that thorough investigation of the continuum, in particular, its part changing quadratically as a function of humidity in this frequency range is of special interest. According to the calculations (see Fig. 13 in [39]) the frequency dependence of the continuum must be different from the quadratic dependence observed at lower frequencies and adopted in propagation models. The hump on the dimer absorption spectrum near 450 GHz clearly seen in Fig. 13 of [39] is most likely caused by the maximum intensity of water dimer rotational spectrum reached in this range at room temperature ($2B \approx 12$ GHz [40]). The dimer spectrum calculations [39] revealed that in the mm range, water dimer absorption alone reproduces the experimentally determined water continuum absorption. Our recent accurate measurements of the continuum [41] confirmed this conclusion. Therefore, accurate investigation of the continuum in the 300–600 GHz range could give additional evidence of the dimer origin of the absorption.

To conclude, the analysis of the obtained broad-band atmospheric spectra confirms a high potential of the resonator method demonstrated in our earlier works and proves that the method is a useful tool for both spectroscopic applications and solution of fundamental problems of molecular physics.

Acknowledgments

The authors are grateful to P.W. Rosenkranz for assistance in modifying the MPM model for this study. We also appreciate the assistance of A. Sutyagin, A. Yakovlev, A. Kiselev and P. Pakhomov in obtaining experimental data at low pressures.

The research was partly supported by the RFBR and by the Russian Federal Special Program "Scientific and Educational Personnel of the Innovative Russia" for 2009-2013.

References

[1] Pardo JR, Serabyn E, Cernicharo J. Submillimeter atmospheric transmission measurements on Mauna Kea during extremely dry El Nino conditions: implications for broadband opacity contributions. J Quant Spectrosc Radiat Transfer 2001;68:419–33.

[2] Seta T, Hoshina H, Kasai Y, Hosako I, Otani C, Lossow S, et al. Pressure broadening coefficients of the water vapor lines at 556.936 and 752.033 GHz. J Quant Spectrosc Radiat Transfer 2008;109:144–50.

[3] Bauer A, Godon M, Duterage B. Self- and air-broadened linewidth of the 183 GHz absorption in water vapor. J Quant Spectrosc Radiat Transfer 1985;33:167–75.

[4] Bauer A, Godon M, Kheddar M. Temperature and perturber dependences of water vapor 380 GHz-Line broadening. J Quant Spectrosc Radiat Transfer 1987;37:531–9.

[5] Goyette TM, De Lucia FC. The pressure broadening of the $3_{1,3}$–$2_{2,0}$ transition of water between 80 and 600 K. J Mol Spectrosc 1990;143:346–58.

[6] Colmont J-M, Priem D, Wlodarczak G, Gamache RR. Measurements and calculations of the halfwidth of two rotational transitions of water vapor perturbed by N_2, O_2, and air. J Mol Spectrosc 1999;193:233–43.

[7] Tretyakov MYu, Parshin VV, Shanin VN, Myasnikova SE, Koshelev MA, Krupnov AF. Real atmosphere laboratory measurement of the 118-GHz oxygen line: shape, shift, and broadening of the line. J Mol Spectrosc 2001;208:110–2.

[8] Tretyakov MYu, Parshin VV, Koshelev MA, Shanin VN, Myasnikova SE, Krupnov AF. Studies of 183-GHz water line: broadening and shifting by air, N_2 and O_2 and integral intensity measurements. J Mol Spectrosc 2003;218:239–45.

[9] Golubiatnikov GYu, Krupnov AF. Microwave study of the rotational spectrum of oxygen molecule in the range up to 1.12 THz. J Mol Spectrosc 2003;217:282–7.

[10] Tretyakov MYu, Golubiatnikov GYu, Parshin VV, Koshelev MA, Myasnikova SE, Krupnov AF, et al. Experimental study of line mixing coefficient for 118.75 oxygen line. J Mol Spectrosc 2004;223:31–8.

[11] Tretyakov MYu, Koshelev MA, Dorovskikh VV, Makarov DS, Rosenkranz PW. 60-GHz oxygen band: precise broadening and central frequencies of fine structure lines, absolute absorption profile at atmospheric pressure, revision of mixing coefficients. J Mol Spectrosc 2005;231:1–14.

[12] Golubiatnikov GYu. Shifting and broadening parameters of the water vapor 183-GHz line (3_{13}–2_{20}) by H_2O, O_2, N_2, CO_2, H_2, Ne, Ne, Ar and Kr at room temperature. J Mol Spectrosc 2005;230:196–8.

[13] Koshelev MA, Tretyakov MYu, Golubiatnikov GYu, Parshin VV, Markov VN, Koval IA. Broadening and shifting of the 321-, 325- and 380-GHz lines of water vapor by the pressure of atmospheric gases. J Mol Spectrosc 2007;241:101–8.

[14] Tretyakov MYu, Koshelev MA, Koval IA, Parshin VV, Kukin LM, Fedoseev LI, et al. Temperature dependence of pressure broadening of 1-oxygen line at 118.75 GHz. J Mol Spectrosc 2007;241:109–11.

[15] Golubiatnikov GYu, Koshelev MA, Krupnov AF. Pressure shift and broadening of 1_{10}–1_{01} water vapor lines by atmosphere gases. J Quant Spectrosc Radiat Transfer 2008;109:1828–33.

[16] Makarov DS, Koval IA, Koshelev MA, Parshin VV, Tretyakov MYu. Collisional parameters of the 118-GHz oxygen line: temperature dependence. J Mol Spectrosc 2008;252:242–3.

[17] Makarov DS, Tretyakov MYu, Rosenkranz PW. 60-GHz oxygen band: precise experimental profiles and extended absorption modeling in a wide temperature range. J Quant Spectrosc Radiat Transfer 2011;112:1420–8.

[18] Koshelev MA. Collisional broadening and shifting of the 2_{11}–2_{02} transition of $H_2^{16}O$, $H_2^{17}O$, $H_2^{18}O$ by atmosphere gases. J Quant Spectrosc Radiat Transfer 2011;112:550–2.

[19] Tretyakov MYu, Koshelev MA, Makarov DS, Tonkov MV. Precise measurements of collision parameters of spectral lines with a spectrometer with radioacoustic detection of absorption in the millimeter and submillimeter ranges. Instrum Exp Tech 2008;51:78–88 [Translated from Pribory i Tekhnika Eksperimenta (Rus.) 2008;1:87–98].

[20] Tretyakov MYu, Krupnov AF, Koshelev MA, Makarov DS, Serov EA, Parshin VV. Resonator spectrometer for precise broadband investigations of atmospheric absorption in discrete lines and water vapor related continuum in millimeter wave range. Rev Sci Instrum 2009;80:093106.

[21] Parshin VV, Tretyakov MYu, Koshelev MA, Serov EA. Modern resonator spectroscopy at submillimeter wavelengths. IEEE Sensors J, http://dx.doi.org/10.1109/JSEN.2012.2215315, in press.
[22] Krupnov AF, Tretyakov MY, Parshin VV, Shanin VN, Myasnikova SE. Modern millimeterwave resonator spectroscopy of broad lines. J Mol Spectrosc 2000;202:107–15.
[23] Liebe HJ. MPM—an atmospheric millimeter-wave propagation model. Int J Infrared Mill Waves 1989;10:631–50;
Rosenkranz PW. Water vapor microwave continuum absorption: a comparison of measurements and models. Radio Sci 1998;33: 919–28;
Rosenkranz PW. Water vapor microwave continuum absorption: a comparison of measurements and models. Radio Sci 1999;34:1025.
[24] Gamache RR, Fischer J. Half-widths of $H_2^{16}O$, $H_2^{18}O$, $H_2^{17}O$, $HD^{16}O$, and $D_2^{16}O$:I. Comparison between isotopomers. J Quant Spectrosc Radiat Transfer 2003;78:289–304 Data are available from URL〈http://faculty.uml.edu/Robert_Gamache/〉.
[25] Liebe HJ, Layton DH. Millimeter-wave properties of the atmosphere: laboratory studies and propagation modeling. NTIA report no. 87-224; 1987.
[26] Van Vleck JH, Weisskopf VF. On the shape of collision-broadened lines. Rev Mod Phys 1945;17:227.
[27] Townes CH, Schawlow AL. Microwave spectroscopy. New York: Dover Publications; 1975.
[28] Bubukina II, Zobov NF, Polyansky OL, Shirin SV, Yurchenko SN. Optimized semiempirical potential energy surface for $H_2^{16}O$ up to 26000 cm^{-1}. Opt Spectrosc 2011;110:160–6 [Translated from Optika i Spektroskopiya (Rus.) 2011;110:186–93].
[29] Rothman LS, Gordon IE, Barbe A, Benner DC, Bernath PF, Birk M, et al. The HITRAN 2008 molecular spectroscopic database. J Quant Spectrosc Radiat Transfer 2009;110:533–72. 〈http://www.cfa.harvard.edu/HITRAN/〉.
[30] Golubiatnikov GYu, Markov VN, Guarnieri A, Knoechel R. Hyperfine structure of $H_2^{16}O$ and $H_2^{18}O$ measured by Lamb-dip technique in the 180–560 GHz frequency range. J Mol Spectrosc 2006;240: 191–4.
[31] Meshkov AI, De Lucia FC. Laboratory measurements of dry air atmospheric absorption with a millimeter wave cavity ringdown spectrometer. J Quant Spectrosc Radiat Transfer 2007;108:256–76.
[32] Tretyakov MYu, Golubiatnikov GYu, Parshin VV, Koshelev MA, Krupnov AF. Obtaining precise constants of atmospheric lines in the millimeter and submillimeter wavelength ranges. Radiophys Quant Electron 2008;51:713–7 [Translated from Izv. Vuzov Radiofizika (Rus.) 2008;9:789–94].
[33] Koshelev MA, Markov VN, Vilkov IN. J Quant Spectrosc Radiat Transfer, in preparation.
[34] Hartmann J-M, Boulet C, Robert D. Collisional effects on molecular spectra laboratory experiments and models, consequences for applications. Amsterdam: Elsevier; 2008.
[35] Ngo NH, Tran H, Gamache RR, Hartmann JM. Pressure effects on water vapour lines: beyond the Voigt profile. Philos Trans Roy Soc A 2012;370:2495–508.
[36] Koshelev MA, Tretyakov MYu, Rohart F, Bouanich J-P. Speed dependence of collisional relaxation in ground vibrational state of OCS: rotational behavior. J Chem Phys 2012;136:124316.
[37] Ma Q, Tipping RH, Gamache RR. Uncertainties associated with theoretically calculated N_2-broadened half-widths of H_2O lines. Mol Phys 2010;108:2225–52.
[38] Jacquinet-Husson N, Crepeau L, Armante R, Boutammine C, Chedin A, Scott NA, et al. The 2009 edition of the GEISA spectroscopic database. J Quant Spectrosc Radiat Transfer 2011;112: 2395–445. 〈http://ara.abct.lmd.polytechnique.fr/〉.
[39] Scribano Y, Leforestier C. Contribution of water dimer absorption to the millimeter and far infrared atmospheric water continuum. J Chem Phys 2007;126:234301.
[40] Keutsch FN, Goldman N, Harker HA, Leforestier C, Saykally RJ. Complete characterization of the water dimer ground state and testing of WRT(ASP-W)III SAPT-5st, and VRT(MCY-5f) surfaces. Mol. Phys 2003;101:3477–92.
[41] Koshelev MA, Serov EA, Parshin VV, Tretyakov MYu. Millimeter wave continuum absorption in moist nitrogen at temperatures 261–328 K. J Quant Spectrosc Radiat Transfer 2011;112 2704–1.